Journal of Oceanography, Vol. 64, pp. 103 to 114, 2008

Particle Tracking Experiments on a Model of the Okhotsk Sea: Toward Oil Spill Simulation

KAY I. OHSHIMA[1]* and DAISUKE SIMIZU[2]

[1]*Institute of Low Temperature Science, Hokkaido University, Sapporo 060-0819, Japan*
[2]*Japan Sea National Fisheries Research Institute, Fisheries Research Agency, Niigata 951-8121, Japan*

(Received 27 April 2007; in revised form 13 September 2007; accepted 13 September 2007)

Particle tracking experiments were conducted for the Sea of Okhotsk using a three-dimensional ocean circulation model, as a step toward the simulation of oil spills. The model's reproducibility is first examined in detail. Comparison with surface drifter and moored ADCP data shows that the model successfully reproduces the velocity field over the shelves, particularly in the weak stratification period. This is because the current variability is simply determined by integration of the alongshore component of the wind stress over the coast from which arrested topographic waves propagate. Good agreement even in the ice-covered period implies that the neglect of sea ice in the model is not a problem for reproduction of the current over the shelves. Good agreement also supports the correction of ECMWF wind speed by a factor of 1.25. A series of particle tracking experiments was carried out to examine the case of particles released from the Sakhalin oil field at depths of 0 m and 15 m. Regardless of the deployment month and year, most particles at depth 15 m are transported southward along the Sakhalin coast, in accordance with the abrupt intensification of the East Sakhalin Current in October, finally arriving offshore of Hokkaido in November–January. Particles at the surface, which are affected by wind drift in addition to the ocean current, show larger yearly variability. In years when the offshoreward-wind dominates, the particles would be advected out of the mainstream of the current and would not be transported offshore of Hokkaido.

Keywords:
· Sea of Okhotsk,
· East Sakhalin Current,
· particle tracking,
· spilled oil,
· arrested topographic wave.

1. Introduction

The circulation in the Sea of Okhotsk has been revealed by intensive current measurements carried out in 1998–2001 under the Joint Japanese-Russian-U.S. Study of the Sea of Okhotsk. Surface drifter observations (Ohshima *et al*., 2002) clearly revealed a southward current along the bottom contours over the east Sakhalin shelf, called the East Sakhalin Current (abbreviated as ESC hereafter). The ESC appears to exist as a western boundary current of the cyclonic gyre over the mid-north region of this sea. These features are qualitatively consistent with the old schematics (Watanabe, 1963; Moroshkin, 1966). Ohshima *et al*. (2002) further showed that the ESC consists of two cores: the nearshore core on the shelf and the offshore core over the shelf slope. Mizuta *et al*. (2003) clarified the structure and seasonal variations of the ESC based on long-term moored current measurements. They showed that the total transport of the southward flow at 53°N was 6.7 Sv (1 Sv = 10^6 m^3 s^{-1}) as an annual average, varying from a maximum in winter to a minimum in late summer.

So far several numerical model studies have been done for the circulation in the Sea of Okhotsk (Sekine, 1990; Simizu and Ohshima, 2002, 2006; Watanabe *et al*., 2004; Ohshima *et al*., 2004; Nishi *et al*., 2004; Nakamura *et al*., 2006; Uchimoto *et al*., 2007). Simizu and Ohshima (2002, 2006) showed that the nearshore core (branch) of the ESC is mainly driven by the cross-shore component of Ekman flux trapped over the shelf and can be interpreted as an "Arrested Topographic Wave" (hereafter ATW) (Csanady, 1978). The nearshore core (branch) also includes a component that is a surface intensified current due to the fresh water flux from the Amur River, although this component is seasonal and has small transport (Mizuta *et al*., 2002). On the other hand, Ohshima *et al*. (2004)

* Corresponding author. E-mail: ohshima@lowtem.hokudai.ac.jp

showed that the offshore core (branch) of the ESC can be regarded as the western boundary current of the cyclonic circulation driven by a positive wind stress curl.

The Sea of Okhotsk is the southernmost sea with sizeable seasonal ice cover in the Northern Hemisphere. In winter, sea ice formation begins over the northwestern shelf at the end of November, and ice extent becomes maximum in late February or March, covering 50–90% of the whole sea. Most of the ice disappears by May.

Exploitation of the Sakhalin shelf gas and oil fields since the 1990s has enhanced the intensity of oil transportation in the Sea of Okhotsk. The risk of oil spill incidents requires a system for monitoring, simulating, and forecasting oil spills. A number of oil spill models are in use in the world today (e.g., Proctor *et al*., 1994; Reed *et al*., 1999). In the neighboring Sea of Japan, a serious oil spill incident occurred from the Russian tanker Nakhodka in January 1997. The spillage of heavy oil from the Nakhodka affected thousands of kilometers of Japan's coastline, causing huge social and economic damage. Motivated by this incident, a series of oil spill simulation models have been developed for the Sea of Japan (Varlamov *et al*., 1999, 2000, 2003). These models are based on a particle tracking method using an ocean general circulation model. The models incorporate wind drift, random diffusion, buoyancy effect, parameterization of oil evaporation, biodegradation, and beaching.

In the Nakhodka incident, cold weather conditions acted to form a very stable, persistent water-in-oil emulsion, which traveled to unusually great distances. Under this condition, ocean currents play an important role in the transport of spilled oil (Varlamov *et al*., 1999). A similar condition applies in the Sea of Okhotsk, so reproduction of the current field is particularly important for oil spill simulation in the Sea of Okhotsk.

In February and March 2006, thousands of dead seabirds were found in massive amounts of oil on the shores of Hokkaido, including part of a UNESCO World Heritage site. Although the cause of this incident has not been clarified, these birds were likely transported from the north via the ESC. If an oil spill incident occurred around the Sakhalin oil field, spilled oil would be brought southward along the Sakhalin coast and finally to Hokkaido by the ESC. Due to the demand for operational simulation, an oil spill simulation model for the Sea of Okhotsk was developed by the Petroleum Association of Japan (2005). Although that model incorporates the effect of wind drift reasonably, the background ocean current in the model is based on schematics from the old Russian and Japanese literature, with no seasonal variation. Considering that the ocean current is the most important component in oil spill simulation with the timescale of a week to several months, a model incorporating the appropriate ocean current is indispensable.

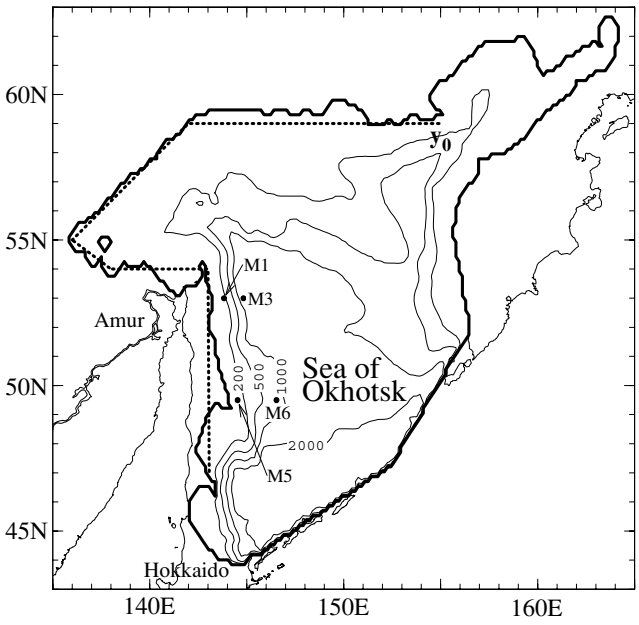

Fig. 1. Model geometry. Thick contours without values denote the model coastline, and thin contours with values give model bottom contours in meters. Dotted lines show the integration route of the wind stress for calculation of the ATW transport. Solid circles denote the mooring locations.

In this study, as a step toward the development of a prediction model for the drift/diffusion of spilled oil in the Sea of Okhotsk, we have conducted a series of particle tracking experiments using the general circulation ocean model of Simizu and Ohshima (2006). We first examine the reproducibility of the model in detail, which is also one purpose of this study. We examine for which regions, seasons, and timescales, and to what degree the model can reproduce the observations. After description of the model, its comparison with the observations, and the method of particle tracking, we present the results of a series of experiments when the particles are released from the Sakhalin oil field, and discuss the results. Our focus is on the simulation with a timescale of a week to several months.

2. Model Description

The model of Simizu and Ohshima (2006), adopted in this study, is a Princeton Ocean Model (POM), primitive equation ocean model with the σ-coordinate in the vertical grid. The model domain includes the entire Okhotsk Sea. Zonal and meridional grid spacings are 1/6°, corresponding to about 11 km and 18.5 km, respectively. Figure 1 shows the model domain with bottom topography, which is based on ETOPO5 data with 5 minute resolution. The model topography is somewhat smoothed

Table 1. Forcing of numerical experiments and comparison with the drifter velocity. Correlation, bias, and standard deviation of the difference (STD) are calculated for the north-south component on a 3-day running mean basis.

Experiment	Wind stress	Heat flux	Amur flux	Correlation	Bias cm/s	STD cm/s
1	daily mean	no	no	0.64	–2.9	11.7
2	daily mean	monthly mean	no	0.75	–1.8	10.1
3	daily mean	monthly mean	monthly mean	0.69	–1.9	10.9

on the shelf slope east of Sakhalin Island to suppress the error in the pressure gradient. The vertical grid uses 21σ levels, with the vertical resolution being finer near the surface. For example, at a typical shelf depth of 100 m, the thicknesses of the uppermost three layers are 0.7 m, 1.5 m, and 2.9 m (see table 1 in Simizu and Ohshima (2006)). The level 2.5 turbulent closure scheme of Mellor and Yamada (1982) is adopted to calculate the vertical eddy viscosity and diffusivity. Therefore, the velocity structure of Ekman flow is realized in the model to some extent, at least over the shelf. In the initial state the ocean is at rest and density stratification is horizontally uniform. The initial temperature and salinity profiles are typical values in the Okhotsk Sea. All straits are closed and thus inflow and outflow are neglected.

Three experiments driven by different heat and salt fluxes were carried out (Table 1). Experiment 1 was run without heat and salt/fresh water flux, experiment 2 was run with the monthly mean heat flux and no salt/fresh water flux, and experiment 3 was run with the heat flux and Amur fresh water flux. The heat flux used in this study is the monthly mean climatology calculated by Ohshima *et al*. (2003). Fresh water flux is given in the north end of Tartar Strait (near the Amur mouth). Climatological monthly means of the Amur discharge from Ogi *et al*. (2001) were used as the flux data. Salt/fresh water fluxes associated with precipitation, evaporation, and sea ice formation/melting were not included because no reliable data are available to us.

For wind data we use the European Centre for Medium-Range Weather Forecasts Re-Analysis data (ERA-40) with latitude and longitude resolution of 1.125°. The daily mean wind stresses are calculated from 6-hourly wind data at 10 m above the sea surface from 1985 to 1999. On the basis of comparison with the Comprehensive Ocean-Atmosphere Data Set (COADS), the ERA-40 wind speed is corrected by a factor of 1.25 for the whole area (Ohshima *et al*., 2003). A similar wind correction was also implemented in the previous models: Simizu and Ohshima (2006) used the factor 1.25, and Simizu and Ohshima (2002) and Uchimoto *et al*. (2007) used the factor 1.30. To calculate wind stress we use a stability-independent drag coefficient following Large and Pond (1981). In winter, although the Okhotsk Sea is partially covered with sea ice, the change in the stress due to the presence of sea ice is not taken into consideration in our model. After integration of 11 years with the climatological monthly mean wind stress, integration of 15 more years with the daily 1985–1999 wind stress was performed for experiments 1 and 2. For experiment 3, only the 1999 case was done.

3. Model Reproducibility

When simulating the drift and diffusion of spilled oil, representation of the currents in the upper 0–15 m layer of the sea is the most important element (Varlamov *et al*., 1999), so reproduction of ocean currents is crucial in the model. The model used in this study (Simizu and Ohshima, 2006) was found to reproduce the observed current field on a monthly mean basis to some extent. Varlamov *et al*. (1999) demonstrated that a model with daily-varying wind forcing that can reproduce realistic current variability is appropriate for representation of the turbulent diffusion of oil. We thus use a model experiment with daily-varying wind forcing. Here we examine the reproducibility of the model on a daily basis. In particular, we examine for which regions and seasons (months) the model has good performance. This provides knowledge of the limitations of the model, which will be useful for designing the particle tracking experiment in the next section.

The surface drifter data obtained in August–December 1999 (Ohshima *et al*., 2002) were used for comparison with the model velocity. The drifter has a large holey sock drogue centered at 15 m depth, and thus it represents the current at a depth of 15 m. Among 18 drifters used in this study, eight were deployed in and around the ESC region, and six upstream of the ESC.

Figure 2 is a map of fit between the drifter and model (experiment 2) velocities on a 3-day running mean basis. The difference vector between the two velocity vectors is calculated. The ratio of the absolute value of the difference vector to that of the drifter velocity vector is then defined as R and categorized into three classes: good fit ($R < 0.5$: indicated by solid circles), moderate fit ($0.5 < R < 1.0$: indicated by open circles), and poor fit ($R > 1.0$: indicated by crosses). The figure shows that the model can roughly reproduce the drifter velocity in the shelf and

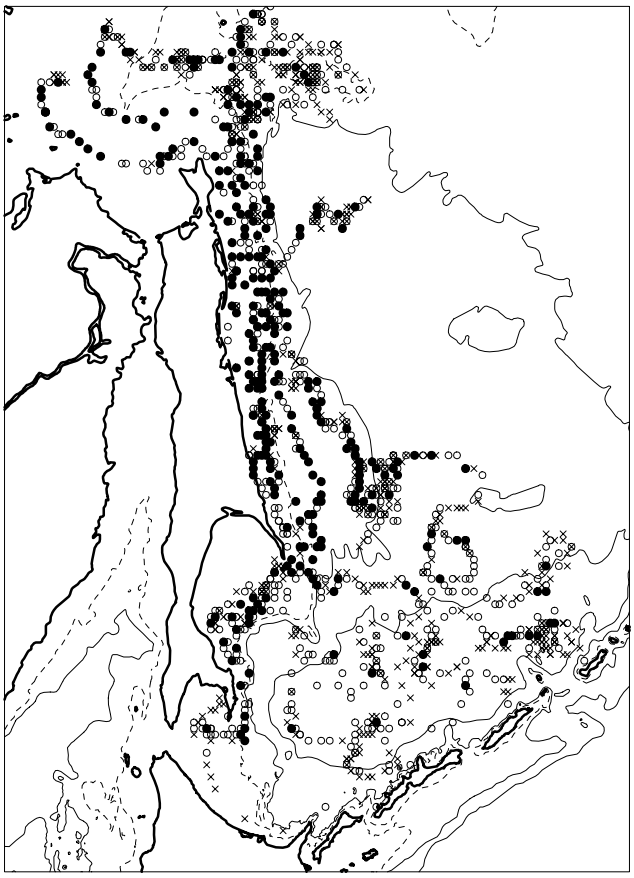

Fig. 2. Map of fit between the model and drifter velocities on a 3-day running mean basis. Good fit ($R < 0.5$: solid circles), moderate fit ($0.5 < R < 1.0$: open circles), and poor fit ($R > 1.0$: crosses). See text for further description. Isobaths at 200 m (dashed lines), 1000 m, 3000 m (thin lines) are also indicated.

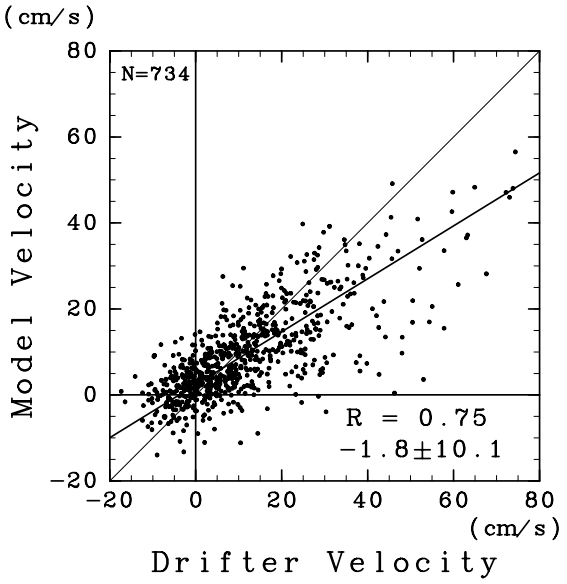

Fig. 3. Scatter plot between the drifter and model north-south velocities in 3-day running mean over the east and north Sakhalin shelves at water depths shallower than 1000 m. Southward direction is taken positive.

slope regions with water depths shallower than 1000 m, but not at all in the deep basin. Figure 3 shows a scatter plot of the drifter and model velocities (north-south component) in 3-day running mean over the east and north Sakhalin shelves with water depths shallower than 1000 m. The model velocity is smaller by 2 cm s^{-1} on average; the standard deviation of the difference between them is ~10 cm s^{-1}. The correlation coefficient between them is 0.75. Although the principal component line shows some bias (see thick line in Fig. 3), the agreement between them is good overall. The model shows relatively good performance in simulating the ESC over the shelves.

Model velocities in the three experiments are compared with the drifter velocity in Table 1. Experiment 2 shows the best agreement. Comparison with the mooring data (not shown) also shows the best agreement with experiment 2. The surface intensified structure of the ESC in summer can be represented in experiment 2 to some degree, but it is not well reproduced in experiment 1. On the other hand, experiment 3 with the Amur River flux cannot adequately represent the component of the density-driven current due to the coarse resolution, as will be discussed later. Experiment 2 is therefore used for particle tracking experiments hereafter.

The next comparison is with the mooring (ADCP) data obtained during 1998–2000 east of Sakhalin Island (see Fig. 1 for the mooring locations). From the correlation coefficient, bias, and standard deviation of the daily north-south velocities between the mooring data and model results (Table 2), we find that M1 and M5 located over the shelf show good correlations, while M3 and M6 located over greater depths show relatively poor correlation. These results are consistent with comparison with drifter observations (Fig. 2).

To check the time-dependent model performance over the shelf, the time series are compared between the model result and the ADCP data at M5. From the surface down to several tens of meters, ADCP records sometimes contain bad data for 6–9 hours per day due to weak echoes caused by vertical migration of scatterers. We therefore used the velocity at 50 m depth for comparison. Figure 4(a) shows the time series of north-south velocity (5-day running mean) at M5 from the model result (blue lines) and the bottom-mounted ADCP (red lines). The model reproduces the observed velocity surprisingly well. Agreement is quite good particularly from January to May, when the density stratification is weak. The southward

Table 2. Comparison of the model velocity (experiment 2) with the ADCP velocity. Correlation, bias, and standard deviation of the difference (STD) are calculated for the north-south component on a daily basis.

Station	Depth m	Level m	Period	Correlation	Bias cm/s	STD cm/s
M1	100	50	Jul. 1998–Nov. 1998	0.84	–8.3	10.6
M1	100	50	Dec. 1998–May 1999	0.87	–6.1	9.3
M5	130	50	Jul. 1998–Nov. 1999	0.74	–4.2	8.8
M5	130	50	Dec. 1998–May 1999	0.70	–0.6	9.6
M3	970	100	Jul. 1998–Sep. 1999	0.56	–8.2	7.7
M6	790	100	Jul. 1998–Dec. 1999	0.49	–1.3	5.6

velocity in the model is somewhat smaller than the observed value from July to November, when the stratification is strong (Table 2), although the model reproduces the observed surface-intensified structure to some extent in these seasons (figure 15 in Simizu and Ohshima (2006)). Note that, even though the model does not include the effect of sea ice, it shows better agreement in the ice-covered period (December–April), which suggests that the inclusion of sea ice in the model is not necessarily important for reproducing the current over the shelf. The model also successfully reproduces the current variability at M1, although the southward component of the modeled velocity is overall smaller than the observed value (Table 2).

Good reproduction in the model suggests that the flow field is determined simply by a certain definite dynamics. Mizuta *et al*. (2005) showed that the variability of the ESC is explained by Coastally Trapped Waves (CTWs). Simizu and Ohshima (2002, 2006), on a monthly data basis, suggested that the seasonal variation of the nearshore branch of the ESC can be explained by Arrested Topographic Waves (ATWs). Both investigations imply that current variability is governed by the alongshore component of the wind stress over the coast from which CTWs or ATWs propagate.

According to Csanady (1978), alongshore volume transport of an ATW is determined by

$$\int_0^\infty V dx' = \int_{y_1}^\infty \frac{\tau_{y'}}{f} dy', \qquad (1)$$

where V is the alongshore component of vertically integrated velocity and a right-handed coordinate system is used with the positive x' axis pointing to the offshore direction and the y' axis lying along the coastline at $x' = 0$. This equation implies that the alongshore transport at y_1 becomes the sum of all backward Ekman transport to or from the coast.

We compare the transport of the nearshore branch at 50°N in the model with the integration of (1) along the dotted lines shown in Fig. 1, where the transport of the nearshore branch in the numerical model is defined as the southward transport integrated from the coast to the region at a water depth of 300 m. The choice of the starting point (y_0) of the integration is based on Simizu and Ohshima (2006): the area east of the starting point ($y_0 < y'$) has complex topography, which gives unfavorable conditions for ATW propagation. Figure 4(b) demonstrates that the volume transport of the nearshore branch of the ESC can be well explained by ATWs even on a daily timescale, as well as on a monthly timescale as shown in Simizu and Ohshima (2006). During August–October, when the stratification is strong, agreement between the model and ATW transports is relatively poor.

During the weak stratification period, when the flow over the shelf is nearly barotropic (Mizuta *et al*., 2003), the velocity at a certain depth is considered to be approximately proportional to the volume transport of the nearshore branch of the ESC. Thus, the integration of the alongshore wind stress is also well correlated with both observed and modeled nearshore velocity (see green lines in Fig. 4(a)) as well as the modeled volume transport. The relatively poor correlation between the observed velocity, modeled velocity, and ATWs in the strong stratification period (July–November) is attributed in part to the fact that the density-driven current by the Amur flux is not included in the model.

In the Sea of Okhotsk, the ESC likely exerts the greatest influence on the drift of particles or spilled oil originating near the coast. Since the observations were limited in area, season, and year, we show the climatology of the ESC from the model on the basis of the 15-year simulations, 1985–1999. Figure 5 shows the monthly mean velocity at a depth of 15 m at M5, averaged over 15 years, with the standard deviation. The ESC shows large seasonal variation, as is also revealed by the observations (Mizuta *et al*., 2003; Ebuchi, 2006). By contrast, the standard deviation for each month is much smaller than the seasonal amplitude: the yearly variation for each month is relatively small. As shown in the next section, the ESC in fall is the most effective component in driving particle

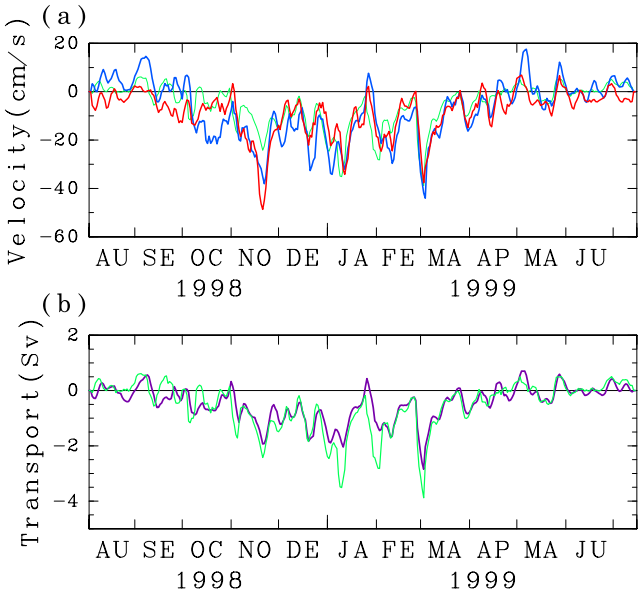

Fig. 4. (a) Time series of velocity at 50 m depth at Station M5 (in Fig. 1) from August 1998 to July 1999, simulated in experiment 2 (blue lines), and measured with the bottom-mounted ADCP (red lines). Volume transport predicted by ATW theory is also superimposed as green lines (scale of left axis is reduced by 1/100 in Sv units). (b) Time series of the nearshore component of ESC transport at 50°N, simulated in experiment 2 (purple lines), and that predicted by ATW theory (green lines). In both panels, 5-day running mean values are plotted and the northward component is positive. 1 Sv = 10^6 m^3 s^{-1}.

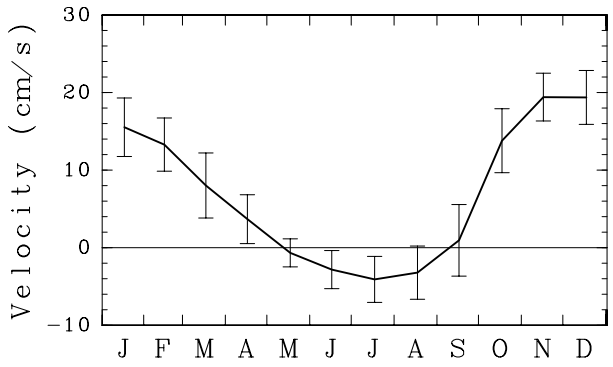

Fig. 5. Monthly variations of simulated velocity at 15 m depth at M5 in experiment 2. North-south component is shown, with southward positive. Values averaged over 15 years (1985–1999) are plotted with standard deviations shown by vertical bars.

drift. Thus we show the detailed velocity structure of the modeled ESC in November, averaged over 15 years (Fig. 6). At a depth of 15 m the current is hardly affected by the wind, while there is a partial wind effect at the surface (Ekman flow), so the current is directed somewhat offshoreward due to the dominant offshoreward wind (see the wind stress vectors designated by green arrows).

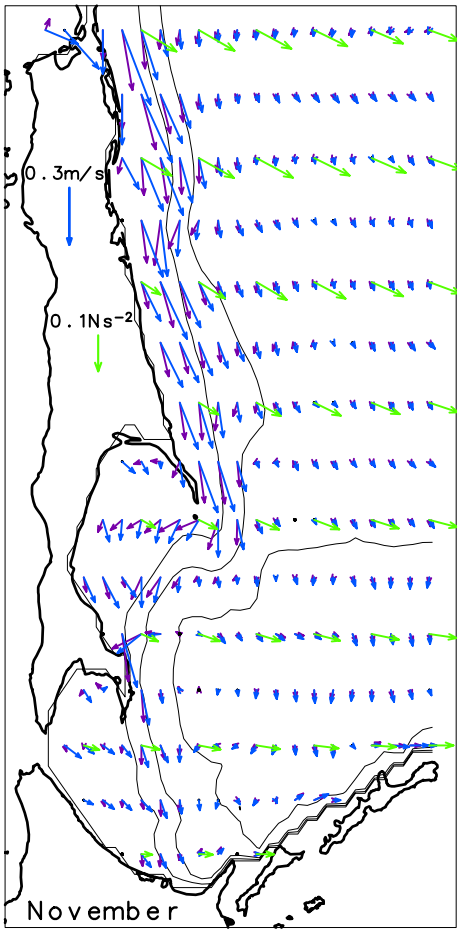

Fig. 6. Simulated velocity vectors at the surface (blue arrows) and 15 m depth (purple arrows) in November, averaged for 15 years in experiment 2. Wind stress vectors (climatology) in November are also superimposed as green arrows. Model coastlines and bottom contours of 200, 500, and 2000 m are denoted by thin lines.

4. Particle Tracking Method

The particle tracking method is similar to that of Awaji (1982). Labeled particles are tracked by the interpolated velocity of the model result. We track the labeled particles at every time step of one-hour Δt ($=t_{m+1} - t_m$), using the calculated Eulerian velocities. The position, $\mathbf{X}_i(t_{m+1})$, of the i-th particle at time t_{m+1} is calculated as:

$$\mathbf{X}_i(t_{m+1}) = \mathbf{X}_i(t_m) + \mathbf{u}'_i(t_m)\Delta t + \int_{t_m}^{t_{m+1}} \left[\mathbf{u}(\mathbf{X}_i(t_m), t) + \int_{t_m}^{t_{m+1}} \mathbf{u}(\mathbf{X}_i(t_m), t') dt' \cdot \nabla \mathbf{u}(\mathbf{X}_i(t_m), t) \right] dt, \quad (2)$$

where **u** denotes an Eulerian velocity at the point of the i-th particle at time t_m, interpolated from Eulerian velocities at four points around the particle. $\mathbf{u}'_i(t_m)$ denotes the turbulent velocity vector experienced by the i-th labeled particle during the time t_m to t_{m+1}. The turbulent velocities are represented by a random-walk in our experiments, assuming a Markov-chain model with a certain horizontal turbulent diffusivity and integral time scale. The method is the same as that described in the appendix in Awaji (1982). According to the Lagrangian statistics from the surface drifter (Ohshima *et al*., 2002), the horizontal turbulent diffusivity was estimated to be of the order of 10^7 cm^2 s^{-1}. This value is probably mainly due to wind-driven variability in a synoptic wind system. This variability has already been included in the model. In our experiments we use 10^6 cm^2 s^{-1} as the horizontal turbulent diffusivity throughout the study. The integral time scale is set to 1 day, which is a somewhat lower value than the estimation by Ohshima *et al*. (2002).

To check the accuracy of this method we ran several tests using shorter time steps for calculating the trajectories, and found that the change of time step gives no significant change. When a particle reaches the coastal boundary, this case is treated as a beaching in the oil spill simulation. Some parameterization is needed for the beaching. In real conditions, this process strongly depends on the character of the coastal zone and the properties of the spilled oil. In this model, however, for such a case, we let the particle remain at the coast at that time step. Because of the effect of random walk diffusion, the particle will soon separate from the coast and drift with the offshore mainstream.

The diffusion mainly comes from the tidal currents over the east Sakhalin shelf north of 51–52°N, where the diurnal shelf (or coastally trapped) waves are excited with amplitude 0.1–0.5 m s^{-1} (Rabinovich and Zhukov, 1984; Ohshima *et al*., 2002). In this study, tidal currents are assumed to be included in the random walk diffusion. For more precise simulation, tidal currents should be included explicitly in the model.

5. Results

We now present the results of the particle tracking experiments in 1998 and 1999, in which good reproduction of the model over the shelves is confirmed by comparison with the observations. The particles are initially placed in a rectangular area that includes the oil field Sakhalin II, shown in Fig. 7. This choice of area is because of the heavy oil transportation traffic and the possibility of an incident in the oil field. The movement and behavior of spilled oil in three-dimensions is rather complex (Varlamov *et al*., 1999). In this study, for simplicity, the particles are assumed to be purely passive tracers at a specified depth. We choose the surface (0 m) and a depth of 15 m for tracking, since the spilled oil is confined mostly to the upper 0–15 m (Varlamov *et al*., 1999). Transformation of the velocity defined in the σ-coordinate to a specified depth is done by linear interpolation or extrapolation. For the surface (0 m), the velocity is determined by extrapolation from the velocities of the uppermost two levels (0.35 m and 1.10 m for the case of 100 m water depth).

Figure 7 shows the simulated time series of particle distribution at (a) the surface and (b) 15 m depth when particles are released every day in October 1998. Since the southward ESC is very strong during October–December, the deployed particles are transported to the region offshore of Hokkaido via the ESC in about two months. Movement of the particle at a depth of 15 m is mostly determined by the ocean current, while that at the surface is somewhat affected by "wind drift", as shown in Fig. 6. The term "wind drift" is used for the drift due to the surface Ekman flow hereafter. Dominance of the northwesterly wind in fall (Fig. 6) causes the surface particles to drift offshore. Thus, the particle distribution at the surface is shifted offshoreward as compared to a depth of 15 m.

Figure 8 shows the simulated particle distribution in the case of June deployment in the same year, 1998. During June–September the ESC is very weak and the mean wind is also weak with northward direction. Thus, the particles at 15 m depth, the drift of which is determined by the ocean current, are almost stagnant over the Sakhalin shelf during summer. After October, in accordance with the abrupt intensification of the ESC, the deployed particles start to move southward swiftly, finally reaching the region offshore of Hokkaido in December. Despite being deployed four months earlier, the particles at a depth of 15 m arrive offshore of Hokkaido in a similar time to the case of October deployment (Figs. 7(b) and 8(b)). On the other hand, the particles at the surface are diffused mainly by the wind drift variability due to synoptic disturbances during summer, and have moved out of the ESC mainstream before the onset of the ESC intensification. Thus they cannot be transported to the region offshore of Hokkaido. Clearly, the particle distribution depends strongly on deployment time and depth.

Figure 9 shows the simulated particle distribution for several layers in the case of October deployment in 1999. At depths of 15 m and 50 m, similar to the case of 1998 (Fig. 7(b)), the particles reach the region offshore of Hokkaido in December via the ESC. The effect of the wind drift becomes larger closer to the surface. Accordingly, the particles closer to the surface are shifted more offshoreward. As will be shown, the offshoreward wind in 1999 is larger than in 1998. At the surface, therefore, all of the particles left the ESC mainstream and never reached the region offshore of Hokkaido, which is quite

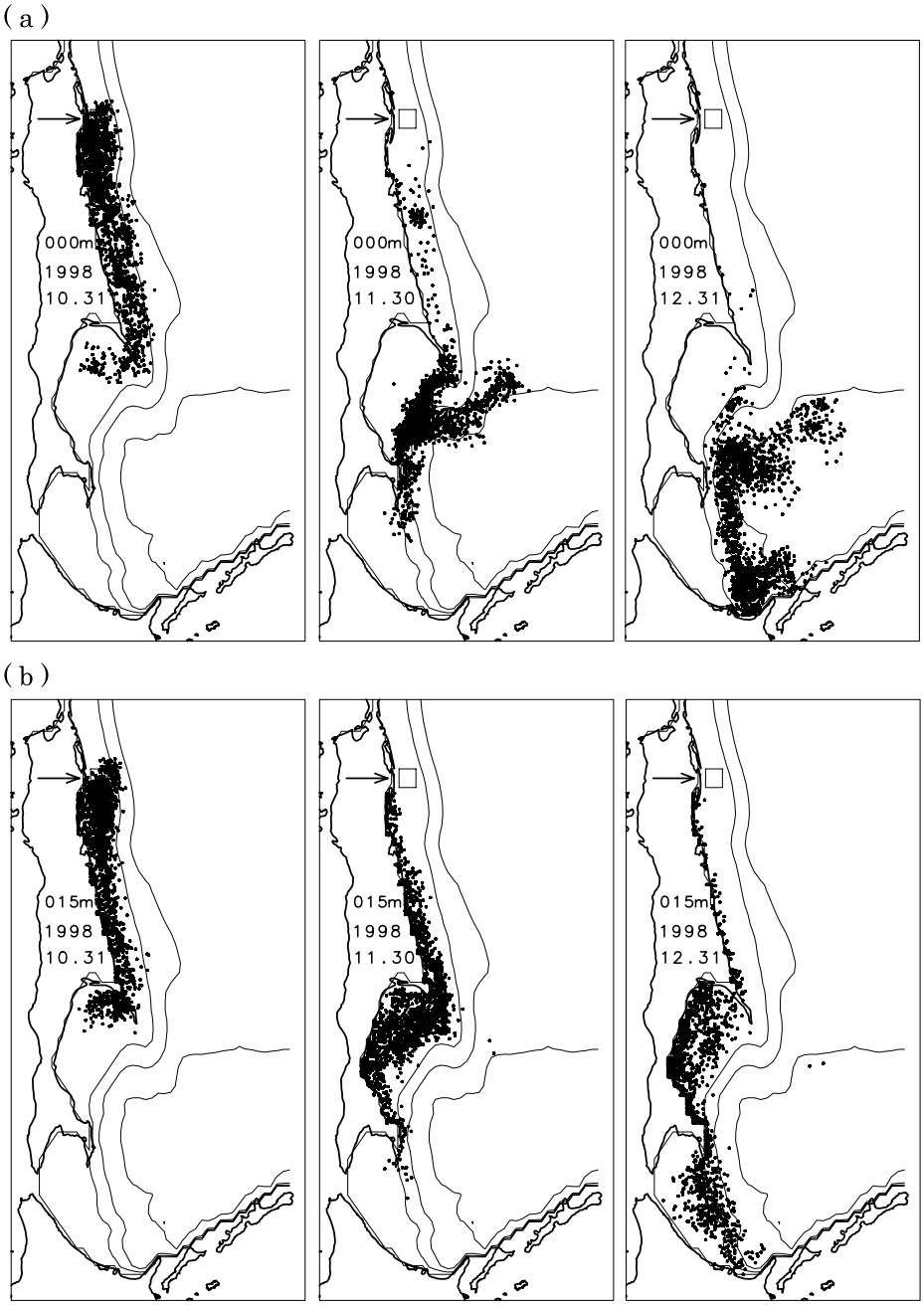

Fig. 7. Simulated time series of particle distribution at (a) surface and (b) 15 m depth at intervals of one month, when 64 particles are released from Sakhalin oil field (designated by arrow and rectangular box) every day in October 1998. Model coastlines and bottom contours of 200, 500, and 2000 m are denoted by thin lines.

different from the 1998 case (Fig. 7(a)). These two cases, 1998 and 1999, suggest that the particle movement at the surface, which is significantly affected by the wind drift, exhibits relatively large yearly differences, while that at a depth of 15 m, which is mostly governed by the sea current with relatively small yearly differences (see Fig. 5), exhibits similar behavior every year.

We have conducted particle tracking experiments for all 15 years (1985–1999) to investigate the means and yearly differences of the drift and diffusion, assuming that the model reproduces the realistic current field to some extent. We divide a one-year cycle into 24 half-month periods. When 64 particles are deployed in the Sakhalin oil field (the rectangular area) every day during each pe-

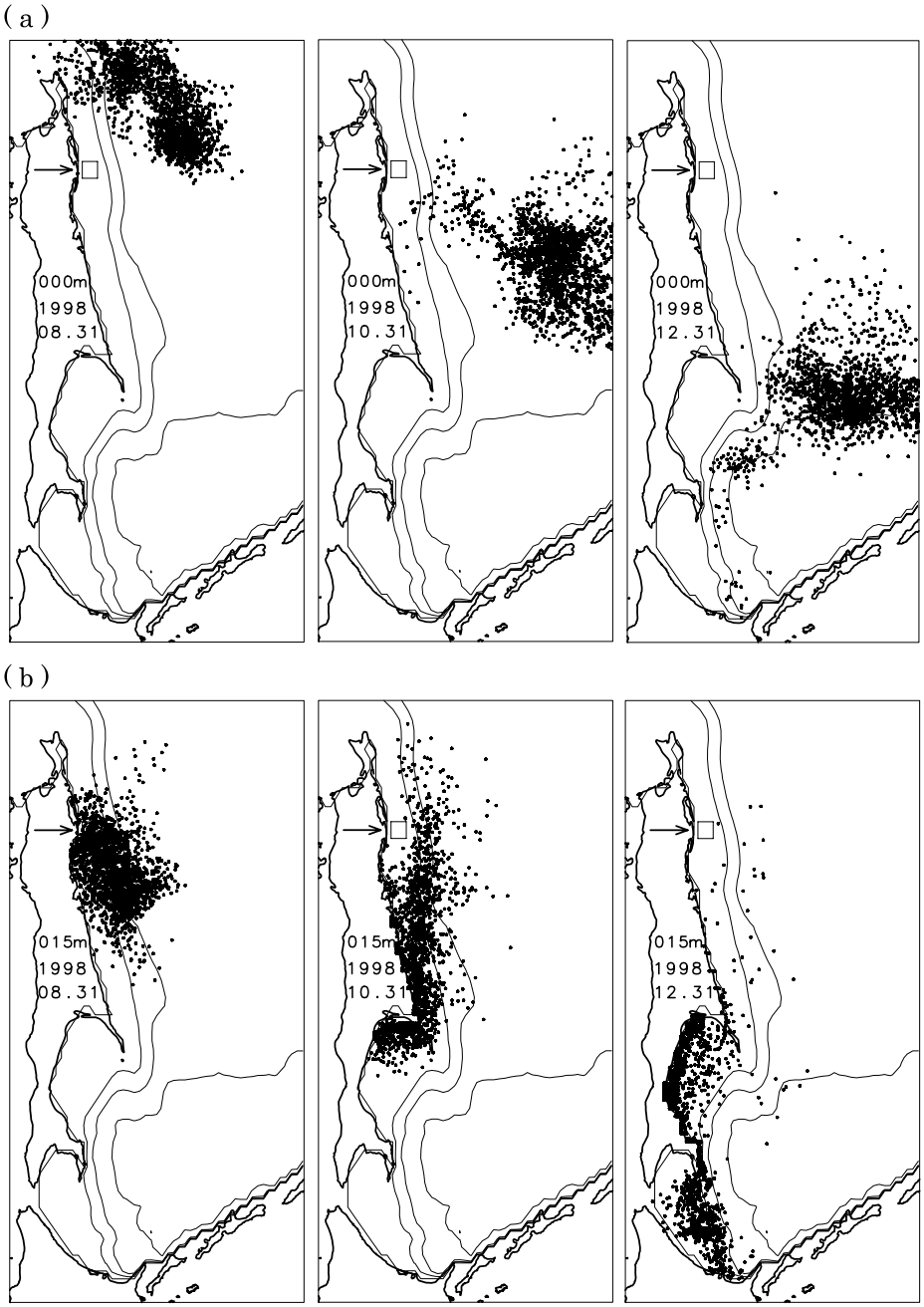

Fig. 8. Simulated time series of particle distribution at (a) surface and (b) 15 m depth at intervals of two months when 64 particles are released from Sakhalin oil field every day in June 1998.

riod, the number of particles that arrive offshore of Hokkaido (south of 45.8°N and west of 145.5°E) is counted on a half-monthly basis. On the basis of experiments for the 15 years 1985–1999, the percentages of particle arrivals are shown as a diagram for the surface (Fig. 10(a)) and 15 m depth (Fig. 10(b)). In accordance with the abrupt intensification of the southward ESC due to onset of the northwesterly monsoon in October or November, particles at a depth of 15 m arrive offshore of Hokkaido around December, regardless of deployment month (Fig. 10(b)). For surface particles, however, this holds only in late summer and fall deployment cases. In the cases of spring and early summer deployment, because of diffusion and/or offshore advection by the wind variability, most of the particles move out of the ESC mainstream and cannot be transported offshore of

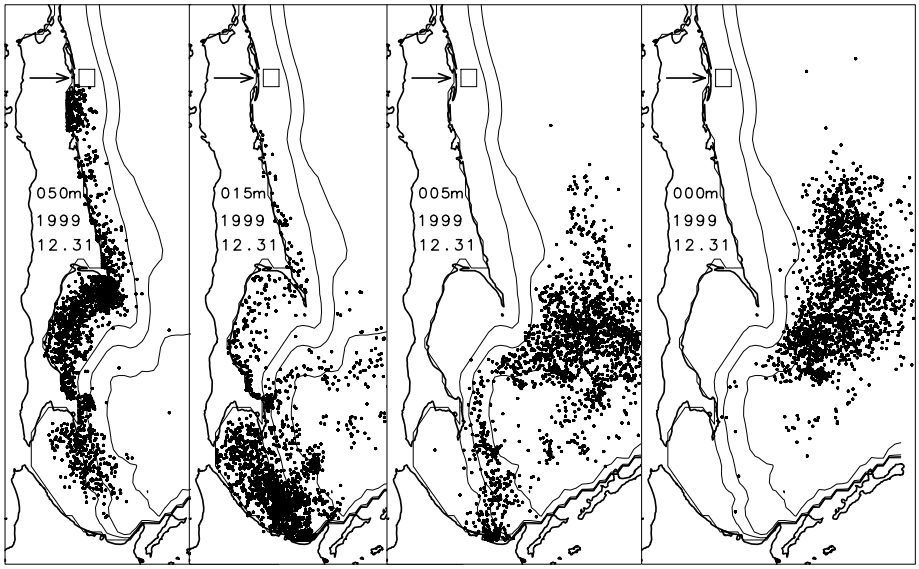

Fig. 9. Simulated particle distributions at surface, 5 m depth, 15 m depth, and 50 m depth, on 31 December 1999, when 64 particles are released from Sakhalin oil field every day in October 1999.

Hokkaido. Regardless of the deployment month, most particles (more than 80%) finally reach the region offshore of Hokkaido at a depth of 15 m, where particle drift is mostly determined by the ocean current, while some or most particles cannot reach Hokkaido at the surface, where wind drift cannot be neglected.

In one year (e.g. 1998), most of the particles released at the surface in fall (October) are transported offshore of Hokkaido, but none reaches Hokkaido in a different year (e.g. 1999). To examine what determines such a yearly difference, we show the yearly difference in percentage of particles that arrive offshore of Hokkaido by the end of the following January among those released in the Sakhalin oil field in October, along with the cross-shoreward (westward) wind stress at M5 (Fig. 11). Among the 1st to 5th largest number of years for particle arrival, 4 years (1988, 1992, 1995, and 1998) are the 1st to 4th smallest years of offshoreward wind. This suggests that whether the surface particle is transported to the Hokkaido coast or not is mostly determined by the cross-shoreward wind component. The only exception is 1989, when the southward ESC (dotted lines in Fig. 11) is strongest among the 15 years. In this year, southward advection by the ESC is strong enough to keep the surface particles in the mainstream, overcoming the offshore drift due to the wind.

6. Summary and Discussion

As a step toward spilled oil simulation of an incident around the Sakhalin oil field, we conducted a series of particle tracking experiments using a general ocean circulation model. Before the particle tracking experiments, we examined the reproducibility of the model in detail. Focusing on the east Sakhalin shelf region, the model successfully reproduces the velocity field including synoptic variability (Figs. 2 and 4; Table 2). In particular, reproducibility is excellent for the weak stratification period, even including the ice-covered period. The neglect of sea ice in the model does not appear to be a problem for reproduction of the current over the shelves. Such high reproducibility is obtained because the flow field is simply determined by ATW dynamics: the volume transport or current variability is governed by integration of the alongshore component of the wind stress (and thus cross-shore Ekman transport) over the coast from which CTWs or ATWs propagate. Good agreement also supports the correction of ECMWF wind speed by a factor of 1.25, done in this study. Without the correction, the southward velocity would be reduced by about one-third. Alternatively, one might consider that the factor 1.25 arises from the stress amplification by sea ice. If so, the southward current in the model would be overestimated during the ice-free period (November). The fact is not as shown in Fig. 4. Thus it is unlikely that the factor 1.25 is a result of amplification by sea ice. For simulation over the ESC region of the shelf, the particle tracking experiments are considered to provide reliable results.

We did particle tracking experiments in which the particles are released from the Sakhalin oil field at depths of 0 m and 15 m, between which most of the spilled oil would be contained. At 15 m depth, particle drift is mostly determined by the ocean current (ESC). The nearshore branch of the ESC, driven by the alongshore wind stress,

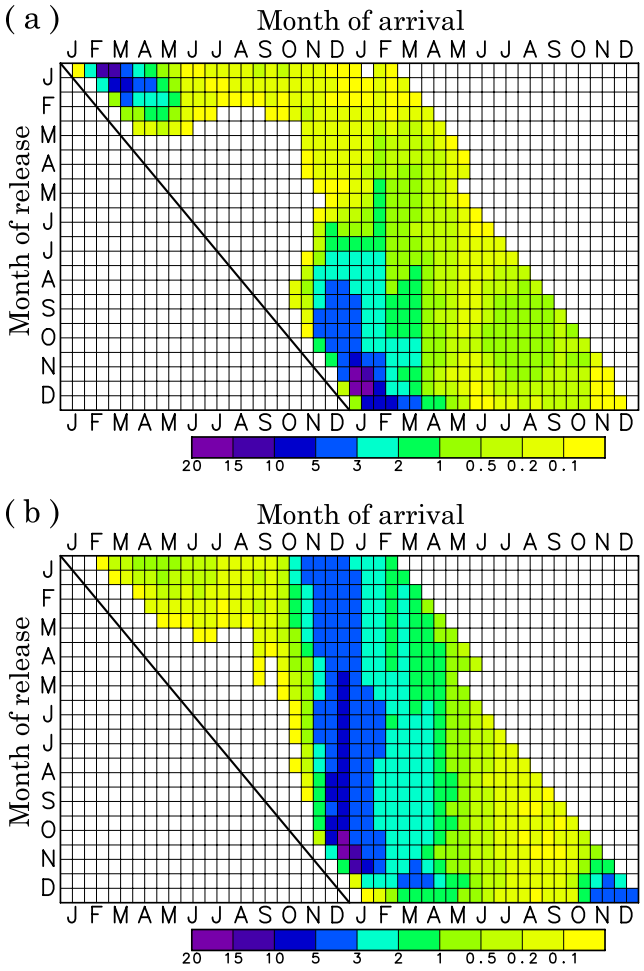

Fig. 10. Diagram for seasonal variation of particle arrival from Sakhalin oil field to the region offshore of Hokkaido (south of 45.8°N and west of 145.5°E) at (a) surface and (b) 15 m depth, based on 15 experiments for 1985–1999. See text for further description.

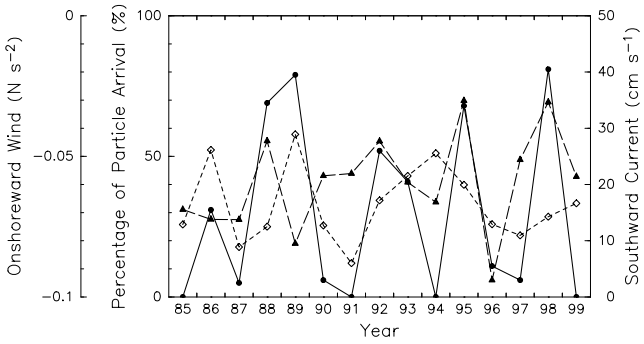

Fig. 11. Yearly differences in (solid lines) percentage of particles that arrive offshore of Hokkaido (defined as in Fig. 10) by the end of January among those released at Sakhalin oil field in the preceding October, (dashed lines) cross-shoreward wind stress at M5 with onshoreward (westward) positive, and (dotted lines) southward component of surface current at M5.

shows large seasonal variations and relatively small yearly differences. Regardless of the deployment month and year, most particles are transported southward along the east Sakhalin coast, in accordance with the abrupt intensification of the ESC in October, finally reaching the region offshore of Hokkaido in November–January (Figs. 7(b), 8(b), and 10(b)). On the other hand, at the surface, particle drift is also affected by wind drift in addition to the ocean current (Fig. 6). The yearly difference in the dominant wind direction causes the difference in the offshore transport, determining whether particles are kept in or out of the ESC mainstream (Figs. 7(a) and 9). In the offshoreward-wind dominant years the particles would not be transported offshore of Hokkaido, even for October deployment (Fig. 11). Particle drift at the surface is more sensitive to the yearly difference in the wind and thus shows larger yearly variability than that at 15 m depth.

This study is a first step towards the simulation of oil spills in the Okhotsk Sea. The spilled oil or particles are treated as passive tracers for the specified depth of water. In reality, the movement and behavior of spilled oil is rather complex. For more realistic simulation, the model should incorporate the effects of wind drag on floating pollutants, the wind stirring effect, the buoyancy effect, parameterization of oil evaporation, biodegradation, and beaching, as in Varlamov *et al*. (1999).

In November 2005, the Amur River was severely polluted by contaminants from a chemical plant explosion. If such contaminants flowed out from the mouth of the Amur River and were dissolved or suspended in sea water, they would be transported southward with the ESC and eventually reach the Hokkaido coast. The particle tracking method used in this study is also effective in simulating the drift of such contaminants.

Although the model shows good performance over the shelf regions, the southward velocity in the model is somewhat underestimated during July–November, when the stratification is strong. This is partly because the density-driven current due to the Amur River flux is not included. Since the internal Rossby radius of deformation is typically 5–10 km in summer in this region, our model, with its resolution of 11–18 km, cannot adequately represent the current driven by the fresh water flux. This inability causes even worse performance in experiment 3, which has fresh water flux (see Table 1). This is why we use experiment 2 for the particle tracking experiment throughout the study. Any future simulation will require a finer resolution model that can resolve the density-driven current, with reliable fresh water/salt flux conditions. For precise simulation near the Hokkaido coast,

inclusion of the inflow (Soya Current) from Soya (La Perouse) Strait is indispensable. A future model should include the water exchange with the Japan Sea and North Pacific. Recently, Uchimoto *et al*. (2007) developed an Okhotsk Sea model with finer resolution and water exchange. Finally, the simulation should take account of the tidal currents, which would play an important role in the diffusion of particles or spilled oil. Such improved model simulations are now under investigation.

Acknowledgements

We would like to thank Masaaki Wakatsuchi, Yasushi Fukamachi, and Genta Mizuta for their encouragement and support. Thanks are extended to Jun Ono, Kazuya Ono, and Kyoko Kitagawa for their help in drawing the figures. Comments by anonymous reviewers helped improve the paper. Figures were produced by the GFD DENNOU Library. KO was supported by a Grant-in-Aid for Scientific Research (17310002) and RR2002 of the Project for Sustainable Coexistence of Human, Nature and the Earth of MEXT of the Japanese Government.

References

Awaji, T. (1982): Water mixing in a tidal current and the effect of turbulence on tidal exchange through a strait. *J. Phys. Oceanogr*., **12**, 501–514.

Csanady, G. T. (1978): The arrested topographic wave. *J. Phys. Oceanogr*., **8**, 47–62.

Ebuchi, N. (2006): Seasonal and interannual variations in the East Sakhalin Current revealed by TOPEX/POSEIDON altimeter data. *J. Oceanogr*., **62**, 171–183.

Large, W. G. and S. Pond (1981): Open ocean momentum flux measurements in moderate to strong winds. *J. Phys. Oceanogr*., **11**, 324–336.

Mellor, G. L. and T. Yamada (1982): Development of a turbulence closure model for geophysical fluid problem. *Rev. Geophys. Space Phys*., **20**, 851–875.

Mizuta, G., Y. Fukamachi, K. I. Ohshima and M. Wakatsuchi (2003): Structure and seasonal variability of the East Sakhalin Current. *J. Phys. Oceanogr*., **33**, 2430–2445.

Mizuta, G., K. I. Ohshima, Y. Fukamachi and M. Wakatsuchi (2005): The variability of the East Sakhalin Current induced by winds over continental shelf and slope. *J. Mar. Res*., **63**, 1017–1039.

Moroshkin, K. V. (1966): Water masses of the Sea of Okhotsk. Joint Pub. Res. Serv., 43942, 98 pp., U.S. Dept. of Commerce, Washington, D.C.

Nakamura, T., T. Toyoda, Y. Ishikawa and T. Awaji, (2006): Enhanced ventilation in the Okhotsk Sea through tidal mixing at the Kuril Straits. *Deep-Sea Res*., **53**, 425–448.

Nishi, Y., S. Tabeta and M. Fujino (2004): Numerical modeling for the seasonal variation of physical oceanographic field of the surface layer in the Okhotsk Sea. *Umi no Kenkyu*, **13**, 37–59 (in Japanese).

Ogi, M., Y. Tachibana, F. Nishio and M. A. Danchenkov (2001): Dose the fresh water supply from the Amur River flowing into the Sea of Okhotsk affect sea ice formation? *J. Meteor. Soc. Japan*, **79**, 123–129.

Ohshima, K. I., M. Wakatsuchi, Y. Fukamachi and G. Mizuta (2002): Near-surface circulation and tidal currents of the Okhotsk Sea observed with satellite-tracked drifters. *J. Geophys. Res*., **107**, 3195, doi:10.1029/2001JC001005.

Ohshima, K. I., T. Watanabe and S. Nihashi (2003): Surface heat budget of the Sea of Okhotsk during 1987–2001 and the role of sea ice on it. *J. Meteor. Soc. Japan*, **81**, 653–677.

Ohshima, K. I., D. Simizu, M. Itoh, G. Mizuta, Y. Fukamachi, S. C. Riser and M. Wakatsuchi (2004): Sverdrup balance and the cyclonic gyre in the Sea of Okhotsk. *J. Phys. Oceanogr*., **34**, 513–525.

Petroleum Association of Japan (2005): Diffusion/drift prediction model for spilled oil: the Okhotsk Sea Version. Ver. 7.1, Users Manual (in Japanese).

Proctor, R., R. A. Flather and A. J. Elliott (1994): Modelling tides and surface drift in the Arabian Gulf-application to the Gulf oil spill. *Cont. Shelf Res*., **14**, 531–545.

Rabinovich, A. B. and A. Ye. Zhukov (1984): Tidal oscillations on the shelf of Sakhalin Island. *Oceanology*, **24**, 184–189.

Reed, M., O. Johansen, P. J. Brandvik, P. Daling, A. Lewis, R. Fiocco, D. Mackay and R. Prentki (1999): Oil spill modeling towards the close of the 20th century: overview of the state-of-the-art. *Spill Science and Technology Bulletin*, **5**, 3–16.

Sekine, Y. (1990): A barotropic numerical model for the wind-driven circulation in the Okhotsk Sea. *Bull. Fac. Bioresources, Mie Univ*., **3**, 25–39.

Simizu, D. and K. I. Ohshima (2002): Barotropic response of the Sea of Okhotsk to wind forcing. *J. Oceanogr*., **58**, 851–860.

Simizu, D. and K. I. Ohshima (2006): A model simulation on the circulation in the Sea of Okhotsk and the East Sakhalin Current. *J. Geophys. Res*., **111**, C05016, doi:10.1029/2005JC002980.

Uchimoto, K., H. Mitsudera, N. Ebuchi and Y. Miyazawa (2007): Anticyclonic eddy caused by the Soya Warm Current in an Okhotsk OGCM. *J. Oceanogr*., **63**, 379–391.

Varlamov, S. M. and J.-H. Yoon (2003): Operational simulation of oil spill in the Sea of Japan. *Rep. Res. Inst., Appl. Mech. Kyushu Univ*., **S1**, 15–20.

Varlamov, S. M., J.-H. Yoon, N. Hirose, H. Kawamura and K. Shinohara (1999): Simulation of the oil spill processes in the Sea of Japan Sea with regional ocean circulation model. *J. Mar. Sci. Technol*., **4**, 94–107.

Varlamov, S. M., J.-H. Yoon, H. Nagaishi and K. Abe (2000): Japan Sea oil spill analysis and quick response system with adaptation of shallow water ocean circulation model. *Rep. Res. Inst. Appl. Mech. Kyushu Univ*., **118**, 9–22.

Watanabe, K. (1963): On the reinforcement of the East Sakhalin Current preceding to the sea ice season off the coast of Hokkaido; Study on the sea ice in the Okhotsk Sea (IV). *Oceanogr. Mag*., **14**, 117–130.

Watanabe, T., M. Ikeda and M. Wakatsuchi (2004): Thermohaline effects of the seasonal sea ice cover in the Sea of Okhotsk. *J. Geophys. Res*., **109**, C09S01, doi:10.1029/2003JC001905.